

Stochastic synchronization of neurons: the topological impacts

Saurabh Kumar Sharma¹, Md. Zubair Malik^{1*}, R.K. Brojen Singh^{1*}

¹School of Computational & Integrative Sciences, Jawaharlal Nehru University, New Delhi-110067, India; R.K. Brojen Singh - E-mail: brojen@jnu.ac.in; Md. Zubair Malik - E-mail: mzubair@jmi.ac.in; *Corresponding authors

Received October 24, 2018; Revised November 17, 2018; Accepted November 18, 2018; Published December 9, 2018

doi: 10.6026/97320630014504

Abstract:

Cross-talk among coupled stochastic Hindmarsh–Rose (HR) neurons is significantly affected by the topology of the neurons organization. If the coupled stochastic HR neurons are arranged in the form of ring topology with odd number of neurons, the neurons are in anti-phase synchronization with homogeneous distribution of phase ordering of the oscillators. On the other hand, if the coupled HR oscillators are arranged in the ring topology with even number of oscillators, the oscillators are formed into two groups which are anti-phase synchronized, but all the oscillators in each group are in in-phase synchronization. Synchronization of the HR oscillators due to coupling in all topological arrangements is affected by the noise. However, noise can induce optimal coherence of the cross-talked oscillators at a particular value at which signal processing is the most favorable with amplified signal, the phenomenon known as stochastic resonance.

Keywords: neurons organization, Hindmarsh–Rose, Synchronization, amplified signal

Background:

Communication among coupled natural systems could be the origin of emergence of important local and global properties, starting from normal state to chaos, crises, chimera and many other peculiar states. One way to deal with such complicated communication among the systems is to study synchronization among these modeled systems using various coupling mechanisms and explore all possible exhibited properties [1–5]. Further, since noise is an inherent parameter in natural systems, it plays an important role in terms of hindrance in signal processing to protect themselves from unwanted external signals (e.g. disease signal, cancer wave, irradiation etc.) and constructive way (enhance signal detection, amplification of signal etc) known as stochastic resonance [6, 7]. On the other hand, topology of the coupled rhythmic systems also affects the properties of the synchronization [8] which lacks intensive study in this direction. Since mechanisms in living systems are noise driven processes, noise helps in various ways [9–13], starting from molecular to phenotypic level: to survive, stay fit, and for protection from the competing environment. For example, pathogens use noise to create

phenotype diversities to enable to survive in the host [14]; higher level organisms use it for adaptation [15, 16]; cells use it to make important decisions and their fates [9] and various cellular phenotypes [17].

The processes in neuron dynamics comprise of random interaction of ions (Na^+ , K^+ , Ca^{2+}) [18, 19], random closing and opening of ion channels [20], and synaptic inputs from the surrounding neurons [21] and can be modeled using stochastic framework [22]. These stochastic processes trigger random firing of membrane potential and other related variables [23]. Since chaotic nature is one of the important features in brain states, Hindmarsh–Rose (HR) model [19], which is a modified version of Fitzhugh model [24], can be taken as a significant model because the can generate bursting spiking patterns and chaotic behavior that is closely mimic to various physiological states of brain. Even though stochastic formalism of this model is not straightforward, one can model HR model using chemical Langevin equation (CLE) formalism [25]. There have been modifications in CLE formalism based on maintaining positivity of the noise part [26] and complex CLE

formalism [27], but these modifications either missing significant contributions from the system variables or limited to some specific models. One way to rescue from this unphysical meaning of negative molecule numbers is to rescale the variables in the model equations [28] and can construct a meaningful stochastic theory of HR model.

The effect on synchronization by the topology of the coupled HR oscillators is the variation in synchronization threshold of the coupled oscillators [8]. Cross-talk among the neurons can be well studied using the concept of synchronization [2] and is a well-studied phenomenon in deterministic HR model using various

coupling mechanisms like electrical [29, 30] and chemical coupling [31], non-local coupling [8], and memristor synaptic coupling [32]. However, the impact of topology of the coupling neurons and its interplay with noise on the neuron communication are not fully studied. The emergence of interesting phenomena of communication through coherence (CTC) is a phenomenon of neuronal communication through interaction of large number of neurons in a network in brain from the complicated neuronal network might be triggered by the topology of the coupled neurons. We focus on the issue of how topology of the interacting neurons affects the properties of communication among these coupled neurons.

Methodology:

Chemical Langevin equation of Hindmarsh-Rose neuron model:

Hindmarsh-Rose (HR) model [19] is an excitable neuron model [33] and can able to exhibit bursting spiking patterns as well as

$$\frac{d}{dt} H = R(x, y, z; t); \quad H = \begin{bmatrix} x \\ y \\ z \end{bmatrix}; \quad R(x, y, z; t) = \begin{bmatrix} y - ax^3 + bx^2 - z + I_{ex} \\ c - dx^2 - y \\ r[s(x - x_0) - z] \end{bmatrix} \rightarrow (1)$$

where x , y and z are variables corresponding to membrane potential, fast current (due to either Na^+ or K^+ ions) and slow current (corresponding to, Ca^{2+}), respectively. The system parameters are chosen as $a = 1$, $b = 3$, $c = 1$, $d = 5$, $x_0 = -1.6$, $s = 4$, $I_{ex} = 3.25$. Various parameter values of r can exhibit different patterns of the system.

The neuron dynamics can be considered as a stochastic process due to random interaction of various ions (Na^+ , K^+ and Ca^{2+}) inside the neuron system, random diffusion of these ions through ion channels, and driving random external fluctuations. Further, various experiments show that the size of a neuron can be affected by various factors; namely, $Sar1a^R$, siRNA and siRNA + $Sar1a^R$ induced growth in dendritic and axonal lengths by 15%-45% in hippocampal neurons [34], organo phosphorus pesticides suppress the growth of axon and dendrite by 10%-30% in cultured sympathetic neurons of rodent [35], p160ROCK inhibition in cortical actin network stability causes the outgrowth of axon by 20%-40% in mammalian [36], and bursts of depolarizing current induced action potential and blocking of calcium current bring

chaotic nature which may correspond to various neurophysiological states. The HR model system is described by,

$$\frac{d}{dt} H = R(x, y, z; t); \quad H = \begin{bmatrix} x \\ y \\ z \end{bmatrix}; \quad R(x, y, z; t) = \begin{bmatrix} y - ax^3 + x^2(b + 3a\alpha) - x(3a\alpha^2 + 2b\alpha) - z + a\alpha^3 + b\alpha^2 + I_{ex} \\ (c + \alpha - d\alpha^2) - dx^2 + 2dax - y \\ r[s(x - x_0) - z - \alpha] \end{bmatrix} \rightarrow (2)$$

If we keep the same values of all constants in equation (1), the scaled model (2) with $\alpha = 13$, same behavior of x , y , and z can be seen in rescaled model. Now, consider the size of a neuron be V at a temperature T with well-stirred ions (Na^+ , K^+ , Ca^{2+}) then the resulting stochastic dynamics of state vector $H^{[s]} = [X, Y, Z]^{-1}$, where, $X = xV$, $Y = yV$, $Z = zV$. Each term in the three differential equations (2) corresponds to a particular state transition in the neuron given by

about rapid contraction of dendritic spine head causing variation in hippocampal neurons' size [37]. The macroscopic variables x , y , and z can be considered as the manifestation of the mentioned complicated interaction of microscopic ions driven by random environment in the neuron. Since $x \propto \frac{Q}{r}$, with Q as total charge in the neuron, the sign in x indicates the nature of the force. Similarly, since $y \propto \frac{Q}{t}$, the sign in y shows the direction of the net charge flow in the neuron. Now, without loss of generality the variables x and y can be scaled with a scale factor α as ($x \rightarrow x + \alpha$, and $y \rightarrow y + \alpha$) to get rid of negative values involved in these variables [28]. Following this scaling procedure, equation (1) becomes

$$n_1 X + n_2 Y + n_3 Z \xrightarrow{k_i} m_1 X + m_2 Y + m_3 Z \rightarrow (3)$$

where k_i is classical rate constant of i^{th} reaction (3) with reactant and product number state vectors $n_i = [n_1, n_2, n_3]^{-1}$, $m_i = [m_1, m_2, m_3]^{-1}$, and state change vector $v_i = n_i - m_i$.

The propensity function, which can be defined as the probability that the reaction (3) can be fired anywhere in the system [22], can be written as $a_i = c_i h_i$, where h_i is the possible molecular

combinations and c_i is the stochastic rate constant given by $c_i = k_i V^{1-v_i}$. Hence, there are thirteen such reaction channels which are constructed from each term in the model (2) (see Table 1) [22, 38]. Following [25] and defining $\Lambda_j = [H^{[s]}(t), t]$ as the number of times

the j^{th} state change takes place within the time interval $[t, t + \Delta t]$, with $\Delta t > 0$; $\Delta t \ll 1$, chemical Langevin equation of HR model can be derived as given by,

$$H_i^{[s]}(t + \Delta t) = H_i^{[s]}(t) + \sum_{j=1}^M \Lambda_j [H^{[s]}(t), \Delta t] v_{ji}, \quad \text{where } M = 11; \quad i = 1, 2, 3 \quad \rightarrow (4)$$

The equation (4) can be simplified by imposing two important approximations: (1) $\Delta t \rightarrow 0$ limit, where no significant change in state change is likely to occur, and $\Delta a_i \sim 0$. This situation can be achieved when reactant molecular population is large, and Λ_j can be approximated to Poisson random variable $\Lambda_j \rightarrow P_j(a_j, \Delta t)$. (2) $\Delta t \rightarrow$ large limit allows $a_j \gg 1$, and one can approximate $P_j(a_j) \rightarrow$

$N_j(a_j \Delta t, a_j \Delta t)$ (normal random variable). These two conditions can be applied simultaneously at the large population limit [25]. Then, applying $N(m, \sigma^2) = m + \sigma N(0, 1)$, where m and σ are mean and standard deviation, and putting $\frac{H_i^{[s]}(t+\Delta t) - H_i^{[s]}(t)}{\Delta t} \approx \frac{dH_i^{[s]}(t)}{dt}$, we arrive at

$$\frac{dH_i^{[s]}(t)}{dt} = \sum_{j=1}^M v_{ji} a_j [H^{[s]}] + \sum_{j=1}^M v_{ji} \sqrt{a_j [H^{[s]}]} \xi_j; \quad \xi_j = \lim_{t \rightarrow 0} N\left(0, \frac{1}{\Delta t}\right) \quad \rightarrow (5)$$

where ξ_j are noise parameters. Now applying the transition of states in Table 1 to equation (5), and putting $x = X/V$, $y = Y/V$, $z = Z/V$, we arrive at CLE for HR model,

$$\frac{d}{dt} H = R(x, y, z; t) + \frac{1}{\sqrt{V}} G(x, y, z, \xi; t); \quad \text{where } H = \begin{bmatrix} x \\ y \\ z \end{bmatrix} \quad \rightarrow (6)$$

$$R(x, y, z; t) = \begin{bmatrix} y - ax^3 + x^2(b + 3a\alpha) - x(3a\alpha^2 + 2b\alpha) - z + a\alpha^3 + b\alpha^2 + I_{ex} \\ (c + \alpha - d\alpha^2) - dx^2 + 2dax - y \\ r[s(x - x_0) - z - s\alpha] \end{bmatrix}$$

$$G(x, y, z, \xi; t) = \begin{bmatrix} \sqrt{y} \xi_1 - \sqrt{ax^3} \xi_2 + \sqrt{x^2(b + 3a\alpha)} \xi_3 - \sqrt{x(3a\alpha^2 + 2b\alpha)} \xi_4 - \sqrt{z} \xi_5 + \sqrt{a\alpha^3 + b\alpha^2 + I_{ex}} \xi_6 \\ \sqrt{(c + \alpha - d\alpha^2)} \xi_7 - \sqrt{dx^2} \xi_8 + \sqrt{2dax} \xi_9 - \sqrt{y} \xi_{10} \\ \sqrt{rsx} \xi_{11} - \sqrt{z} \xi_{12} - \sqrt{rsx_0 + rs\alpha} \xi_{13} \end{bmatrix}$$

The first term in equation (6) is the deterministic counterpart, and the second term is due to internal noise which scales as $1/\sqrt{V}$.

Table 1: Set of differential equations used in the model

Differential equations	Transition of states	Propensity function
$\frac{dx}{dt} = y - ax^3 + x^2(b + 3a\alpha) - x(3a\alpha^2 + 2b\alpha) - z + a\alpha^3 + b\alpha^2 + I_{ex}$	$Y \xrightarrow{1} X$	Y
	$3X \xrightarrow{\alpha} \phi$	$\frac{1}{3!V^2} aX(X-1)(X-2)$
	$2X \xrightarrow{b+3a\alpha} 3X$	$(b + 3a\alpha)X(X-1)$
	$X \xrightarrow{3a\alpha^2+2b\alpha} \phi$	$X(3a\alpha^2 + 2b\alpha)$
	$Z + X \xrightarrow{X^{-1}} \phi$	\bar{V}
	$\phi \xrightarrow{a\alpha^3+b\alpha^2+I_{ex}} X$	$Y(a\alpha^3 + b\alpha^2 + I_{ex})$
$\frac{dy}{dt} = (c + \alpha - d\alpha^2) - dx^2 + 2dax - y$	$\phi \xrightarrow{(c+\alpha-d\alpha^2)} Y$	$Y(c + \alpha - d\alpha^2)$
	$2X + Y \xrightarrow{dY^{-1}} 2X$	$\frac{1}{2V^2} dX(X-1)$
	$X \xrightarrow{2d\alpha} X + Y$	$2dax$
	$Y \xrightarrow{1} \phi$	Y
$\frac{dz}{dt} = r[s(x - x_0) - z - s\alpha]$	$X \xrightarrow{rs} Z$	rsX
	$Z \xrightarrow{1} \phi$	Z
	$Z \xrightarrow{(srx_0+rs\alpha)Z^{-1}} \phi$	$srx_0 + rs\alpha$

Environmental coupling mechanism of Neurons:

Consider two stochastic HR neurons defined by $H^{[1]} = [x_1, y_1, z_1]^{-1}$ and $H^{[2]} = [x_2, y_2, z_2]^{-1}$. When these two neurons are coupled through a common dynamic environment via membrane potential (x), the mean of the internal noise of the arise from the two neurons is also being associated with the dynamics of the neurons. Then, by using this coupling scheme [39, 40], we have

$$\frac{d}{dt} H^{[1]} = W^{[1]} + \frac{\epsilon_1 k_1}{\sqrt{V}} \begin{bmatrix} 0 \\ 0 \\ \theta \Lambda \end{bmatrix} \quad \rightarrow (7)$$

$$\frac{d}{dt} H^{[2]} = W^{[2]} + \frac{\epsilon_2 k_2}{\sqrt{V}} \begin{bmatrix} 0 \\ 0 \\ \theta \Lambda \end{bmatrix} \quad \rightarrow (8)$$

$$\frac{d\theta}{dt} = -\omega\theta - \frac{\epsilon_2}{M} \sum_{i=1}^M k_i [x_i - \alpha]$$

$$W^{[i]} = R^{[i]} + \frac{1}{\sqrt{V}} G^{[i]}; \quad H_i = \begin{bmatrix} x_i \\ y_i \\ z_i \end{bmatrix}$$

$$\Lambda = \frac{1}{M} \sum_{i=1}^M \Gamma_1^{[i]}; \quad M = 2$$

where ω is damping factor of the decay in environmental dynamics. ϵ_1 and ϵ_2 are feedback strengths to the system and environment respectively. k_1 and k_2 are feedback adjusting parameters to the systems and environment too. Here, environment means the extracellular trafficking of ions experienced by each neuron as a consequence of surrounding neurons.

Detection of synchronization

The following two techniques are considered to detect the synchronization of two coupled systems.

Results and discussions:

Topology of arrangement of the coupled identical HR oscillators affects in various ways. The coupled HR oscillators are arranged in a ring with environmental coupling mechanism assigned among them and coupling is done via slow current due to $Ca^{2+}(z)$ variable and look for possible synchronization among the remaining variables x and y . When the coupled oscillators exhibit in-phase synchronization, the threshold synchronization value (the minimum value of the coupling constant ϵt at which the coupled oscillators just exhibit synchronization) increases as the number of coupled oscillators is increased similar to the reported work in [8]. Noise in the coupled HR systems, however, affects significantly in the rate of synchronization by allowing to increase the threshold synchronization value, which means coupled stochastic HR oscillators need higher value of the threshold synchronization value to exhibit synchronization.

The scenario of synchronization is in different way when the coupled HR oscillators are in anti-phase synchronization and topology of the oscillators play an important role in achieving

Recurrence plot: If $x_1(t)$ and $x_2(t)$ are two variables corresponding to two coupled systems, then the two-recurrence plot (x_1, x_2) can able to characterize the rate of synchronization of the two coupled systems [41]. If the points in the (x_1, x_2) plot are randomly scattered, then the two systems are uncoupled. However, if the points are concentrated along one of the diagonals of the (x_1, x_2) plot, then the systems are either in-phase synchronized, or anti-phase synchronized. The thickness of the points along the diagonal indicates how strong the synchronization can be achieved between the two coupled systems (the thinner the line the stronger is the synchronization).

Cross-correlation function:

The equal-time cross-correlation function of the two variables $x_1(\epsilon, t)$, and $x_2(\epsilon, t)$, corresponding to two coupled systems, with coupling strength ϵ , can be defined as [42]

$$C_{x_1, x_2}(\epsilon) = \frac{\langle x_1 x_2 \rangle - \langle x_1 \rangle \langle x_2 \rangle}{\sigma_1 \sigma_2} \quad \rightarrow (9)$$

where $\sigma_i = [\langle x_i^2 \rangle - \langle x_i \rangle^2]^{1/2}$ and $i = 1, 2$ are standard deviations, where $\langle \dots \rangle$ denotes the time average. Then, this order parameter can characterize synchronization strength of the two coupled oscillators as follows:

$C_{x_1, x_2}(\epsilon) = 1$ (if the two systems are synchronized); $= 0$ (if the two systems are uncoupled); $= -1$ (if the two systems are anti-synchronized)

synchronization. When the number of coupled oscillators is odd, the anti-phase synchronization takes place in such a way that the HR oscillators are arranged by distribution of the oscillators at equal phases (Figure 1). If the coupled number of oscillators is three ($N = 3$), then at $V = 50$ the oscillators will achieve anti-phase synchronization at $\epsilon = 0.7$ with phases $2\pi/3$, so on, such that for $N = N_0$ (odd) and for the same parameter values, the coupled HR oscillators will be in anti-phase synchronization with each oscillator at the phase $\theta_{N_0} = 2\pi/N_0$ (Figure 1). We then increased the value of V i.e. by decreasing noise strength (noise $\eta \propto \frac{1}{\sqrt{V}}$) by taking $V = 500$ with same ϵ , the coupled HR oscillators follows the same trend of anti-phase synchronization with $\theta_{N_0} = 2\pi/N_0$ phase distribution of each synchronized oscillators. In this case strength of synchronization of the coupled HR oscillators is more than the lower value of V i.e. stronger noise system. The anti-synchronization phenomenon is shown by recurrence plot (see the materials and methods) with points along second diagonal (Figure 1 second column) and correlation plot with V (Figure 2 middle row). Now, if the number of oscillators is even, the way how the

coupled HR oscillators exhibit anti-phase synchronization is quite different from the way how odd number of coupled HR oscillators exhibit anti-phase synchronization. In this case, half of the total oscillators $N_e/2$ are in in-phase synchronization, whereas, the other half of the oscillators again shows in-phase synchronization, but these two groups exhibit anti-phase synchronization (Figure 2) with each other.

These in-phase and anti-phase synchronization phenomena are detected by recurrence plots in (x_i, x_j) and $((y_i, y_j) \forall i, j = 1, 2, \dots, N$ (for in-phase synchronization distributions of phase points are along the diagonal, whereas, for anti-phase synchronization the phase points are along the opposite diagonal), and correlation C with V plots (Figure 2). The way how the N_e oscillators are distributed among the two groups is as follows: the alternate oscillators are in the same group, and the two groups are anti-synchronized with phase $= \pi$.

The impact of noise in the rate of synchronization of coupled HR oscillators is quite significant. The coupled HR oscillators could not able to exhibit complete synchronization ($C \rightarrow 1$) because noise fluctuations which can be measured from V . For small value of coupling constant $\epsilon = 0.2$ the oscillators show strong synchronization (both in-phase and out-phase synchronization) at large values of V i.e. significantly low noise in the system. But for significantly large values of ϵ ($\epsilon \geq 0.5$), a peculiar scenario can be seen in the synchronization behavior of the oscillators. The oscillators attains strong synchronization at a particular value of V for a fixed ϵ , and then decreases as V increases. This means that $C \rightarrow C_{max}$ (C_{max} is maximum correlation value for a particular ϵ) and noise strength V_0 , but $C < C_{max}$ for both $V > V_0$ and $V < V_0$, which could be the case of stochastic resonance [6, 7], where signal processing of the coupled HR oscillators show maximum at $V \rightarrow V_0$ (Fig. 2 second row panels). Similar scenario can be seen both in even and odd groups of coupled HR oscillators. Further, the threshold coupling parameter value varies as a function of noise in the system V and follows power law behavior $V \sim \epsilon^{-\alpha}$, where, α is power law exponent with value $\alpha = 2.3$.

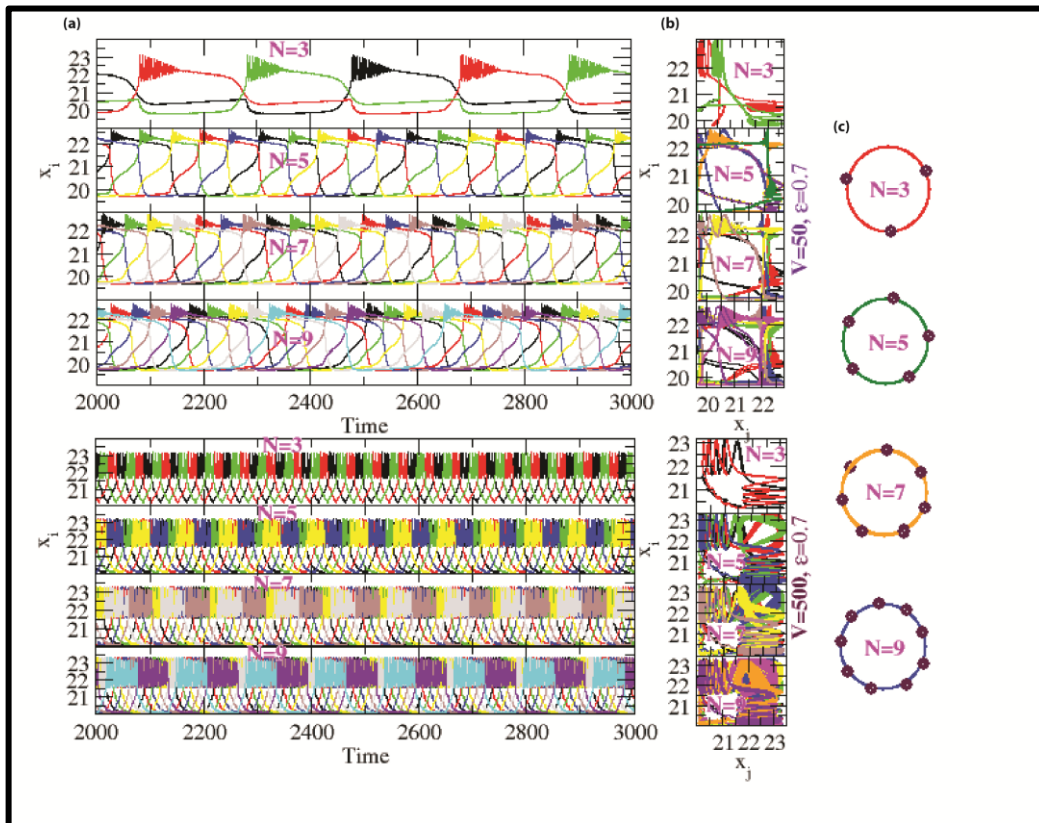


Figure 1: Anti-phase synchronization among odd number of coupled HR oscillators in a ring topology: (a) Dynamics of anti-synchronized $x_i, i = 3, 5, 7, 9$ of coupled HR oscillators for $V = 50, \epsilon = 0.7$ and $V = 500, \epsilon = 0.7$ respectively (left column); (b) Recurrence plots of the coupled HR oscillators showing anti-phase synchronization (second column); (c) Arrangement of coupled HR oscillators with phase distribution (right column).

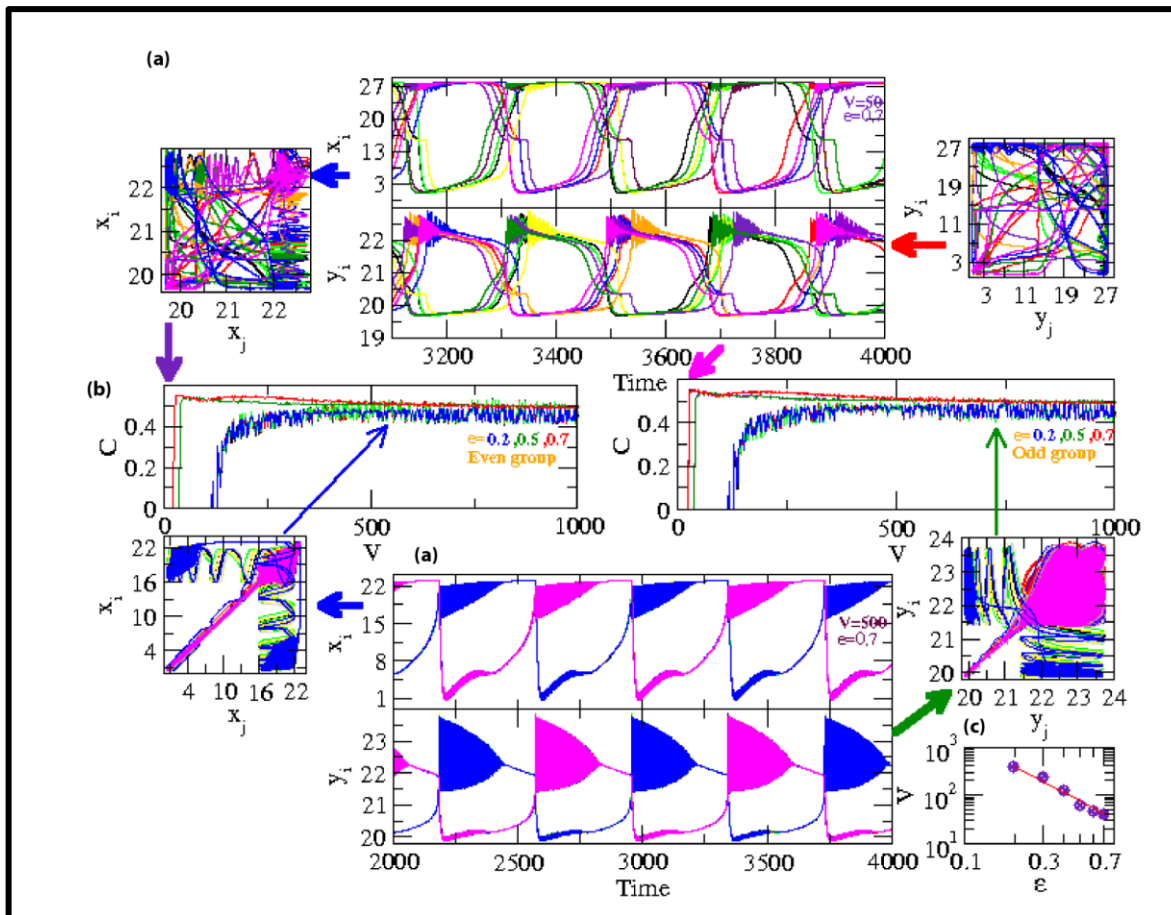


Figure 2: Synchronization of coupled HR oscillators arranged in the form of ring with even number of oscillators: (a) Dynamics of x_i and y_i at $V = 500$ with ϵ values 0.2 and 0.7 respectively (upper and lower panels) with corresponding recurrence plots; (b) Correlation function as a function of V calculated at $\epsilon = 0.2, 0.5, 0.7$ respectively (middle row); (c) Plots of V as a function of ϵ (lower right corner panel).

The synchronization among a coupled stochastic HR oscillator in a certain topology via environmental coupling mechanism is significantly affected by the topology of the network driven by both noise in the system and coupling parameter. When the topology of the oscillators in the ring is odd, each individual in the topology might not be able to arrange in grouping the oscillators, and each individual becomes anti-phase synchrony to every other oscillator. However, if the number of oscillators is even, they might be able to group into two which exhibit anti-phase synchronization. Further, noise could show maximum synchronization at a particular V value which could be the case of stochastic resonance.

Conclusion:

The signal processing among the neurons is affected by various factors and parameters, more importantly by topology of the oscillators under environmental coupling mechanism. The

arrangement of the coupled HR oscillators may trigger different ways of signal processing during the cross-talk among them. When the number of coupled oscillators is odd, grouping into two groups is not possible and hence the situation could be the most favorable case for anti-phase synchronization. The oscillators in each group are in in-phase synchronization, whereas the two groups show anti-phase synchronization. This type of environmental coupling mechanism could be quite possible in multi-neuron cross-talk which could utilize the optimization of signal processing depending on the topology of the neurons network organization to exhibit coherence patterns of cortical neurons in the brain [43]. Noise can be considered as an inherent fundamental parameter in natural systems which is incorporated in the system dynamics, and is very sensitive to the systems, their cross-talk and systems topology. Further, the noise in the system can be related to neuron size, which is quite variable due to both inherent internal and external fluctuations and can be able to

perform both in destructive and constructive ways. This noise can be used to optimize the signal processing in the coupled system generally for fast information processing and signal amplification, the phenomenon known as stochastic resonance. This change in internal noise can also trigger possibilities of cross-talk mechanisms at different neuro physiological states driven by variation in neuron size (mainly axon and dendrite) [34–37]. Coherence due to communication, which can be observed in brain due to interacting neurons, is highly dynamic and very sensitive to noise fluctuations [44]. Moreover, the change in topology with noise in brain stimulus may trigger a drastic change in neurons communication and their functioning. Hence, rigorous theoretical and experimental studies need to be done to observe such phenomena so that one can be able to understand signal processing in brain at fundamental level.

Acknowledgements:

R.K.B.S. is financially supported by Department of Science and Technology (DST), New Delhi, India, under sanction no. SB/S2/HEP-034/2012. M.Z.M. is financially supported by young scientist DHR fellowship, New Delhi, India.

Author contributions:

R.K.B.S conceived the model. R.K.B.S., S.K.S., and M.Z.M. did the numerical experiment. R.K.B.S., S.K.S., and M.Z.M. analyzed, interpreted the simulation results, and wrote the manuscript.

Additional Information:

Competing financial interests: The authors declare no competing interests.

References:

- [1] Glass L. *Nature* **410**: 277284 (2001). [PMID: 11258383]
- [2] Pikovsky A *et al.* Cambridge University Press, 2001.
- [3] Arenas A *et al.* *Phys. Rept.* **469**: 93 (2008).
- [4] Thounaojam US. *et al.* *Eur. Phys. J. Special Topics*, **225**: 17 (2016).
- [5] Thounaojam US. & Shrimali, M.D. *Solitons & Fractals* **107**:5-12 (2018).
- [6] Gammaitoni L *et al.* *Rev. Mod. Phys.* **70**: 223 (1998).
- [7] Hanggi P, *Chem. Phys. Chem.* **3**: 285 (2002). [PMID: 12503175]
- [8] Igor B *et al.* *Phys. Rev. Lett.* **94**: 188101 (2005). [PMID: 15904412]
- [9] Rao CV *et al.* *Nature* **420**: 231 (2002). [PMID: 12432408]
- [10] Samoilov MS *et al.* *Sci. STKE* **366**: 1 (2006). [PMID: 17179490]
- [11] Malik M *et al.* *J. Nanosci Nanotechnol.* **12**: 8303 (2012). [PMID: 23421210]
- [12] Avena-Koenigsberger A *et al.* *Nature Reviews Neuroscience* **19**: 17 (2018).
- [13] Singh SS *et al.* *Journal of theoretical biology* **437**: 58 (2018). [PMID: 28935234]
- [14] Wolf DM *et al.* *J. Theor. Biol.* **234**: 227 (2005). [PMID: 15757681]
- [15] Li Z *et al.* *Genes Dev.* **18**: 1 (2004). [PMID: 14724175]
- [16] Wang CL *et al.* *Proc. Natl. Acad. Sci. U.S.A.* **101**: 7352 (2004). [PMID: 15123833]
- [17] Raj A & van Oudenaarden A, *Cell* **135**: 216 (2008). [PMID: 18957198]
- [18] Hodgkin AL, *J. Physiol.* **107**: 165 (1948). [PMID: 16991796]
- [19] Hindmarsh JL & Rose RM, *Nature* **296**: 162 (1982). [PMID: 7063018]
- [20] White JA *et al.* *Trends Neurosci.* **23**: 131 (2000). [PMID: 10675918]
- [21] Rowat PF & Greenwood PE *Neural Comput.* **23**: 3094 (2011). [PMID: 21919786]
- [22] Gillespie DT, *J. Phys. Chem.* **81**: 2340 (1977). [PMID: 21919786]
- [23] Gerstner W & Kistler WM, *Spiking Neuron Models* (Cambridge University Press, Cambridge, 2002).
- [24] Fitzhugh R, *Biophys. J.* **1**: 445 (1961). [PMID: 19431309]
- [25] Gillespie DT, *J. Chem. Phys.* **113**: 297 (2000).
- [26] Wilkie J & Wong YM, *Chem. Phys.* **353**: 132 (2008).
- [27] Schnoerr D *et al.* *J. Chem. Phys.* **141**: 024103 (2014).
- [28] Poland D *Physica D* **65**: 86 (1993).
- [29] Baptista MS *et al.* *Phys. Rev. E* **82**: 036203 (2010); [PMID: 21230157]
- [30] Guo D *et al.* *Phys. Rev E* **85**: 061905 (2012). [PMID: 23005125]
- [31] Somers D & Kopell N, *Biol. Cybern.* **68**: 393 (1993). [PMID: 8476980]
- [32] Saha DC *et al.* *Ann. Rev. Chaos Theor. Bifur. Dyn. Syst.* **6**: 1 (2016).
- [33] Terman DJ, *Appl. Math.* **15**: 1428 (1991).
- [34] Bing Y *et al.* *Cell* **130**: 717 (2007).
- [35] Howard AS *et al.* *Toxicol. Appl. Pharmacol.* **207**: 112 (2005). [PMID: 6102564]
- [36] Bito H *et al.* *Neuron* **26**: 431 (2000). [PMID: 10839361]
- [37] Eduard K & Segal M, *Neuron* **30**: 751 (2001).
- [38] McQuarrie DA, *J. Appl. Probab.* **4**: 413 (1967).
- [39] Katriel G, *Physica D.* **237**: 2933 (2008).
- [40] Resmi V *et al.* *Phys. Rev. E* **84**: 046212 (2011). [PMID: 22181250]
- [41] Pecora LM & Carroll TL, *Phys. Rev. Lett.* **64**: 821 (1990). [PMID: 10042089]
- [42] Plerou V *et al.* *Phys. Rev. Lett.* **83**: 1471 (1999).
- [43] Michela C *et al.* *Int. J. Neur. Syst.* **17**: 87 (2007). [PMID: 17565505]
- [44] Korn H & Faure P, *C. R. Biol.* **326**: 787 (2003). [PMID: 14694754]

Edited by P Kanguane

Sharma *et al.* *Bioinformation* 14(9): 504-510 (2018)

License statement: This is an Open Access article which permits unrestricted use, distribution, and reproduction in any medium, provided the original work is properly credited. This is distributed under the terms of the Creative Commons Attribution License.